Stem Cell Reports, Volume *16*

Supplemental Information

Engineering spatial-organized cardiac organoids for developmental toxicity testing

Plansky Hoang, Andrew Kowalczewski, Shiyang Sun, Tackla S. Winston, Adriana M. Archilla, Stephanie M. Lemus, A. Gulhan Ercan-Sencicek, Abha R. Gupta, Wenzhong Liu, Maria I. Kontaridis, Jeffrey D. Amack, and Zhen Ma

Supplemental Figures

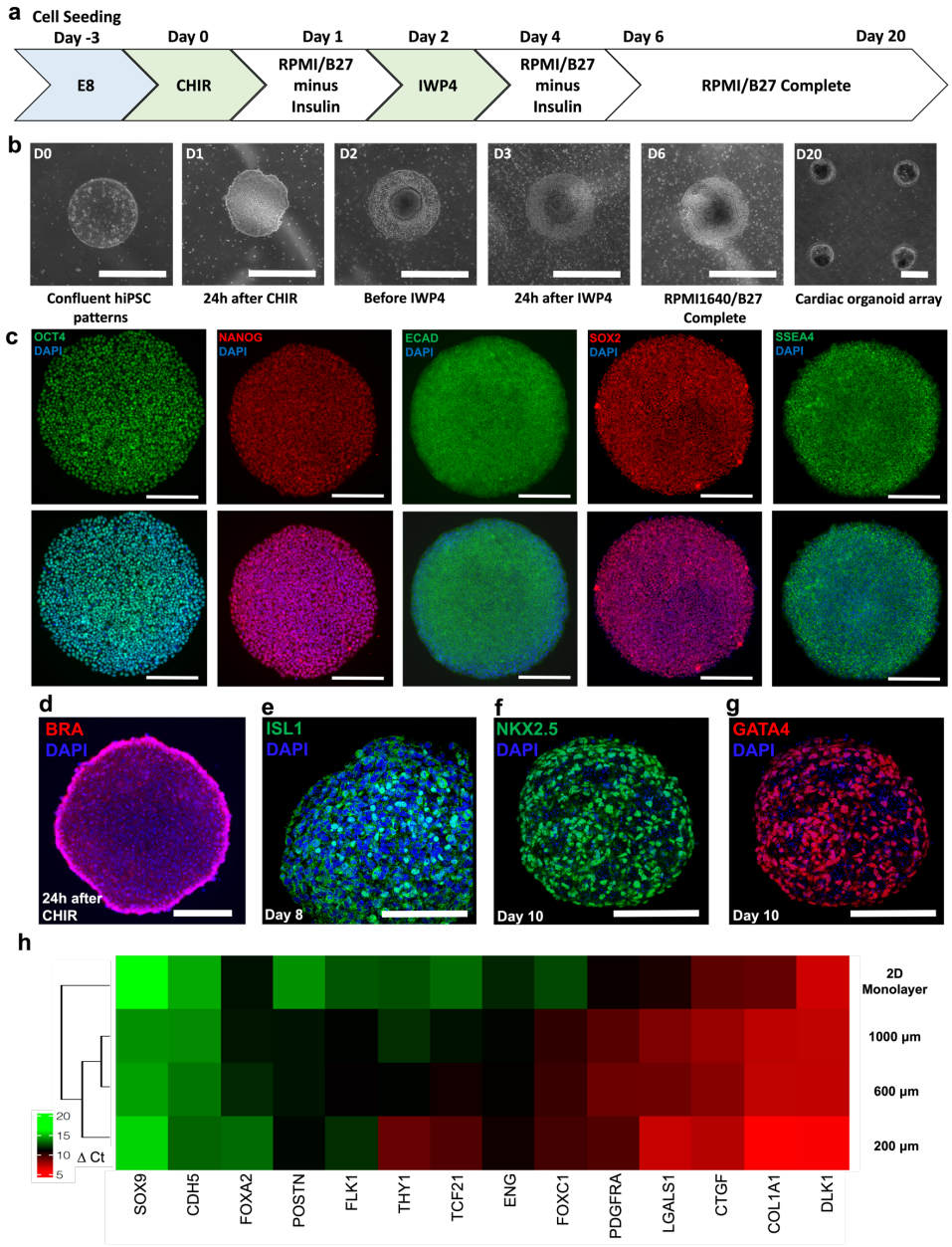

Supplemental Figure 1. *(a) Cardiac differentiation timeline to generate cardiac organoids. (b) Patterned cell morphology changes from 2D monolayer of cells (D0) into 3D tissue (D6 onward) throughout differentiation; scale bars 600 µm. (c) Patterned hiPSCs retain expression of pluripotent markers when confluent (From left to right: OCT4, NANOG, ECAD, SOX2, SSEA4. (d) 24h after CHIR treatment, patterned hiPSCs express mesodermal marker brachyury. (e) On Day 8 of differentiation, cardiac organoids express ISL1, followed by (f) NKX2.5 and (g) GATA4 on Day 10, indicative of early cardiac progenitor cells. (h) Stromal gene expression illustrates higher upregulation of stromal markers in organoids relative to 2D monolayer differentiation and higher upregulation of stromal cell makers in 200-µm organoids relative to 600-µm and 1000-µm organoids. ΔCt values were calculated relative to the average Ct of GAPDH and 18S housekeeping controls. Scale bars 200 µm.*

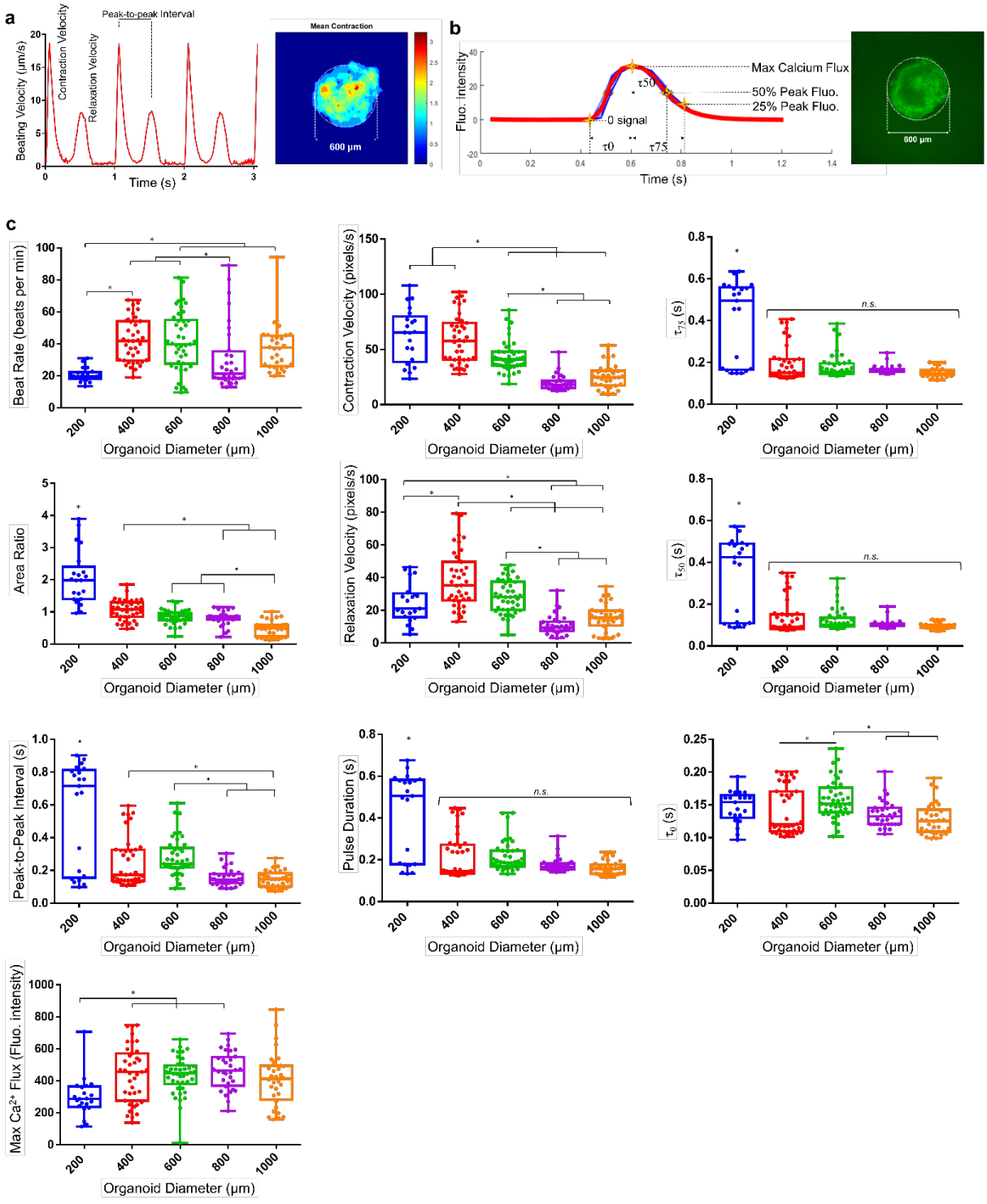

Supplemental Figure 2. *Contraction function analysis of cardiac organoids generated from GCaMP6f hiPSCs. Videos of beating organoids were characterized with using motion tracking analysis to generate (a) motion waveform where each double-peak represents a contraction-relaxation cycle. The Peak-to-peak interval describes the time between the contraction and relaxation peaks. (b) Transient calcium flux signals were acquired from capturing videos of GCaMP6f cardiac organoids and plotting z-axis profiles using ImageJ. Fluorescence bleaching (descending blue*

signal) was corrected (red signal) using in-house MATLAB scripts. Time decay parameters τ_0, τ_{50}, and τ_{75} were acquired by measuring time intervals from the signal initiation to the maximum calcium flux (τ_0), for the maximum flux to decay to 50% (τ_{50}), and for the maximum flux to decay to 25% (τ_{75}). All figures represent schematic illustrations of characterization parameters. (c) Raw data metrics used for data mining and tSNE clustering of organoid contraction functions. Individual points for each variable are shown to illustrate sample distribution. Comparable trends are seen where small patterns significantly prolong the beat duration, based on metrics τ_{75}, τ_{50}, peak-to-peak interval and pulse duration. This can be correlated to the area ratio, which is also significantly greater in small 200 μm organoids. Moreover, most variables illustrated some degree of pattern size dependency, with the most significant functional variations seen in 200 μm organoids. All statistics analyzed using ANOVA with Tukey multiple comparison tests. $p \leq 0.05$ is considered significant (*).

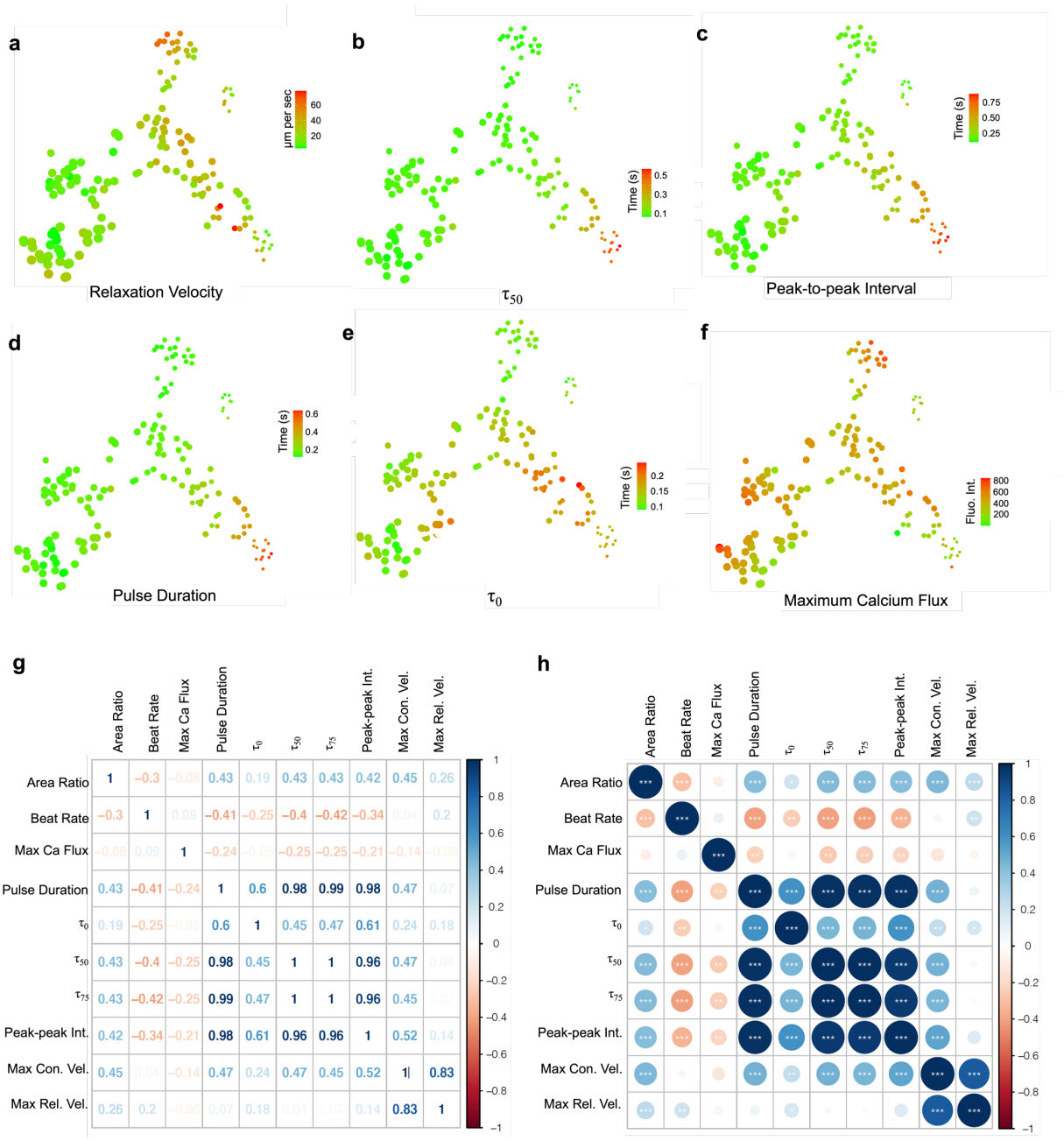

Supplemental Figure 3. *t-SNE gradient plots of contraction functions of cardiac organoids. Contraction function was plotted using co!or gradients to illustrate the influence of organoid size on (a) relaxation velocity, (b) τ_{50}, (c) peak-peak-interval, (d) pulse duration, (e) τ_0, and (f) maximum calcium flux. Small organoids primarily exhibited longer contraction duration cycles, as indicated by higher values in relaxation velocity, τ_{50}, peak-to-peak interval, and pulse duration. All organoids exhibited comparable patterns of maximum calcium flux, indicating that size did not impair the cardiac organoid ability to attain peak contraction. (g) Correlation coefficients showing individual variables correlation with other variable. A correlation coefficient closer to 1 is equivalent to positive correlation, where negative correlation is associated with values close to -1. (h) P-value representation of correlation coefficient significance. (*) denotes $p \leq 0.05$; (**) denotes $p \leq 0.01$; (***) denotes $p \leq 0.001$.*

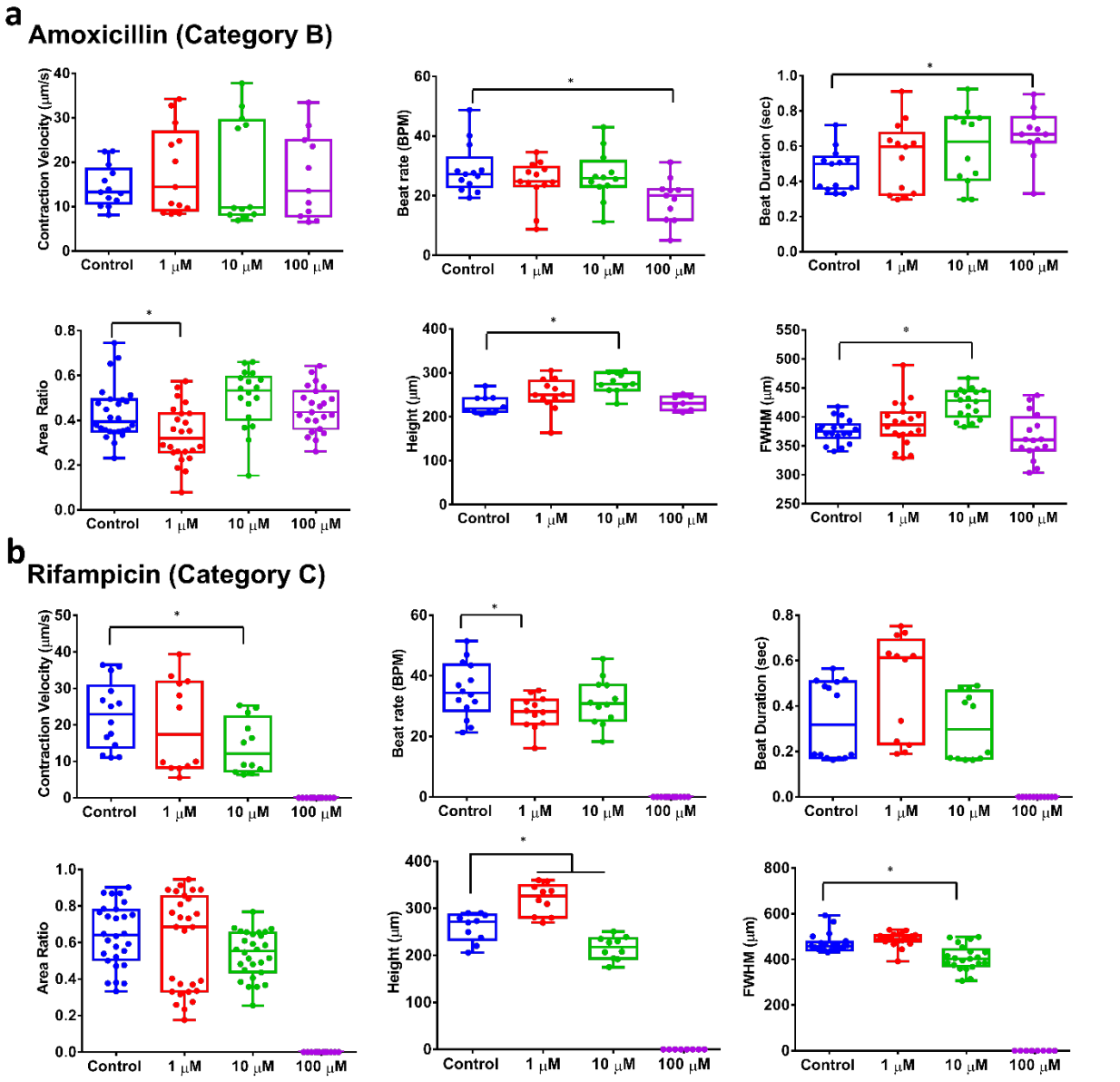

Supplemental Figure 4. *Developmental toxicity assay of cardiac organoids in response to treatment with Category B and C drugs. (a) Amoxicillin showed moderate toxicity with decreased beat rate (ANOVA, n ≥ 11, *p = 0.0215) and increased beat duration (ANOVA, n ≥ 11, *p = 0.0484) at high concentrations. Amoxicillin treatment at low concentrations, however, produced smaller cardiac tissues in area ratio (ANOVA, n ≥ 18, *p = 0.0003 between Controls and 1 μM), height (ANOVA, n ≥ 7, *p = 0.0006), and FWHM (ANOVA, n≥16, *p ≤ 0.0001). (b) Developmental toxicity assay of cardiac organoids in response to treatment with Category C drug, Rifampicin. In all assays, cardiac organoids failed to differentiate at 100 μM treatment, and toxicity was also observed in contraction velocity (ANOVA, n ≥ 12, *p <0.0001), beat rate (ANOVA, n ≥ 12, *p < 0.05), height (ANOVA, n ≥ 10, *p ≤ 0.05) and in FWHM (ANOVA, n ≥ 21, *p < 0.05).*

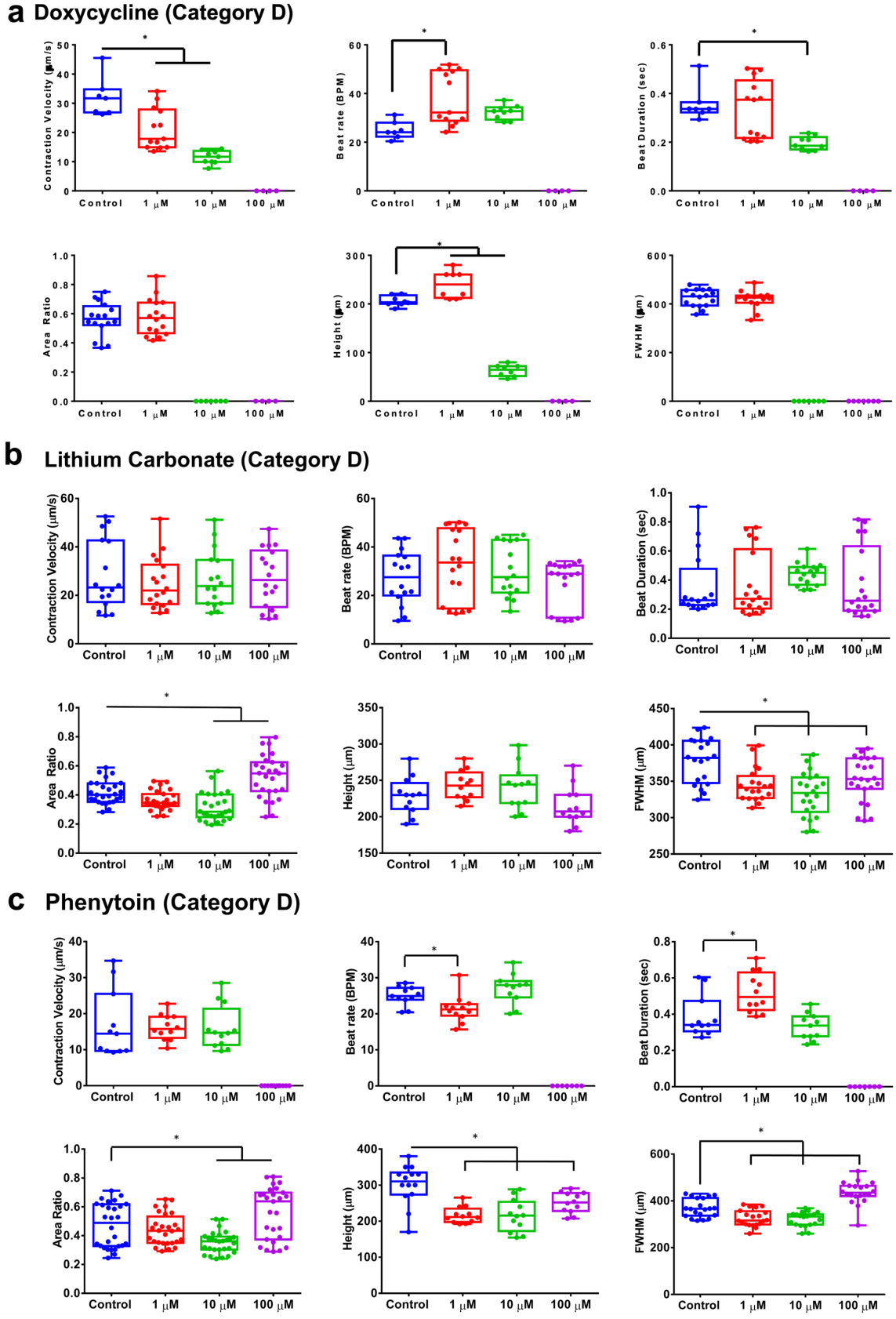
a Doxycycline (Category D)
Contraction Velocity (μm/s)
Beat rate (BPM)
Beat Duration (sec)
Area Ratio
Height (μm)
FWHM (μm)
b Lithium Carbonate (Category D)
Contraction Velocity (μm/s)
Beat rate (BPM)
Beat Duration (sec)
Area Ratio
Height (μm)
FWHM (μm)
c Phenytoin (Category D)
Contraction Velocity (μm/s)
Beat rate (BPM)
Beat Duration (sec)
Area Ratio
Height (μm)
FWHM (μm)
Control
1 μM
10 μM
100 μM
*

Supplemental Figure 5. *Developmental toxicity assay of cardiac organoids in response to treatment with Category D drugs. (a) With doxycycline treatment, cardiac organoids failed to differentiate at 100 μM treatment, and did not form robust cardiac tissues at 10 μM. Significant toxicity was observed in contraction velocity (ANOVA, $n \geq 7$, $^*p < 0.05$), beat rate (ANOVA, $n \geq 7$, $^*p < 0.05$), beat duration (ANOVA, $n \geq 7$, $^*p \leq 0.0001$), and height (ANOVA, $n = 8$, $^*p$ 0.05 relative to controls) and in FWHM (ANOVA, $n \geq 21$, $^*p < 0.05$). (b) With lithium carbonate treatment, no significant toxicity effects were seen in any contraction function. However, moderate toxicity was seen in higher concentrations for the area ratio (ANOVA, $n \geq 26$, $^*p \leq 0.0001$) and in FWHM (ANOVA, $n \geq 20$, $^*p \leq 0.0001$) relative to the controls. (c) Phenytoin showed no contractile functions at 100 μM concentration, with moderate effects at 1 μM on beat rate (ANOVA, $n \geq 11$, $^*p < 0.0001$) and beat duration (ANOVA, $n \geq 11$, $^*p < 0.0001$). Organoids were also smaller in area ratio at 10 μM treatment (ANOVA, $n = 28$, $^*p < 0.0001$) and smaller at all concentrations in height (ANOVA, $n \geq 12$, $^*p \leq 0.0001$) and at low and moderate concentrations in FWHM (ANOVA, $n=20$, $^*p \leq 0.0001$) relative to controls.*

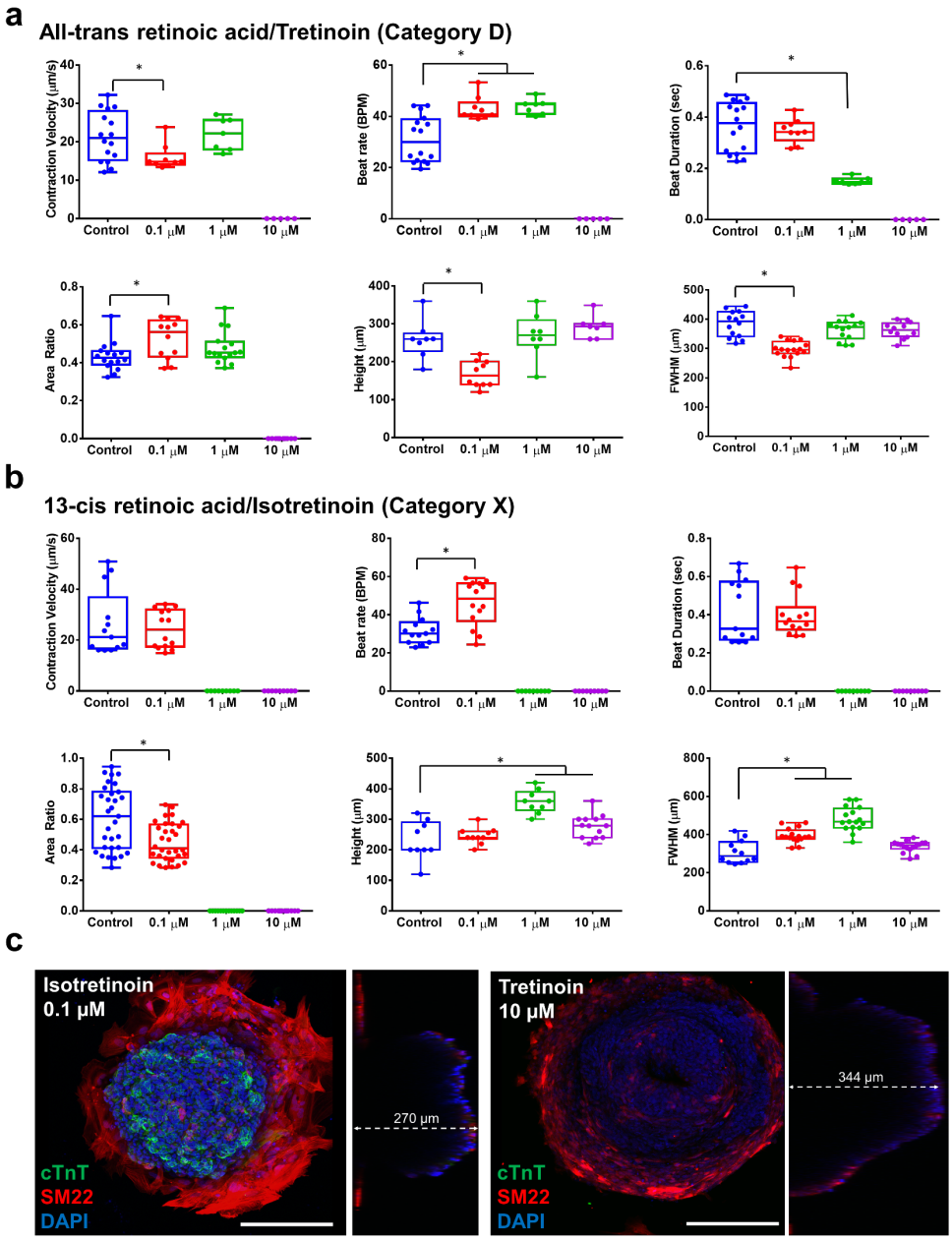

Supplemental Figure 6. *Developmental toxicity assay of cardiac organoids in response to treatment with retinoids Tretinoin (Category D) and Isotretinoin (Category X). (a) With tretinoin, cardiac tissue failed to differentiate at 10 μM concentrations with no contraction functions. Contraction velocity was lower at 0.1 μM (ANOVA, $n \geq 7$, $^*p < 0.0001$), whereas beat rate was faster at 0.1μM and 1 μM (ANOVA, $n \geq 7$, $^*p < 0.0001$). Beat duration was significantly lower at 1 μM (ANOVA, $n \geq 7$, $^*p \leq 0.0001$) as well. Low concentration of 0.1 μM also showed toxic effects on area ratio (ANOVA, $n \geq 12$, $^*p \leq 0.0001$), height (ANOVA, $n \geq 8$, $^*p < 0.0001$), and FWHM (ANOVA, $n \geq 12$, $^*p \leq 0.0001$). (b) Cardiac tissue failed to develop at 1 μM and 10 μM concentrations with no contraction functions. Low concentration of 1 μM resulted in faster beat rate (ANOVA, $n \geq 13$, $^*p \leq 0.0001$) and smaller area ratio (ANOVA, $n \geq 31$, $^*p \leq 0.0001$). However, high concentrations produced organoids that were significantly taller in height (ANOVA, $n \geq 9$, $^*p \leq 0.0001$) and larger in FWHM (ANOVA, $n \geq 12$, $^*p \leq 0.0001$). (c) Representative images show cardiac tissue formation at low (0.1 μM) concentration, but a large mound with no cardiac tissue at high (10 μM) concentration of retinoid exposures. Scale bars 200 μm.*

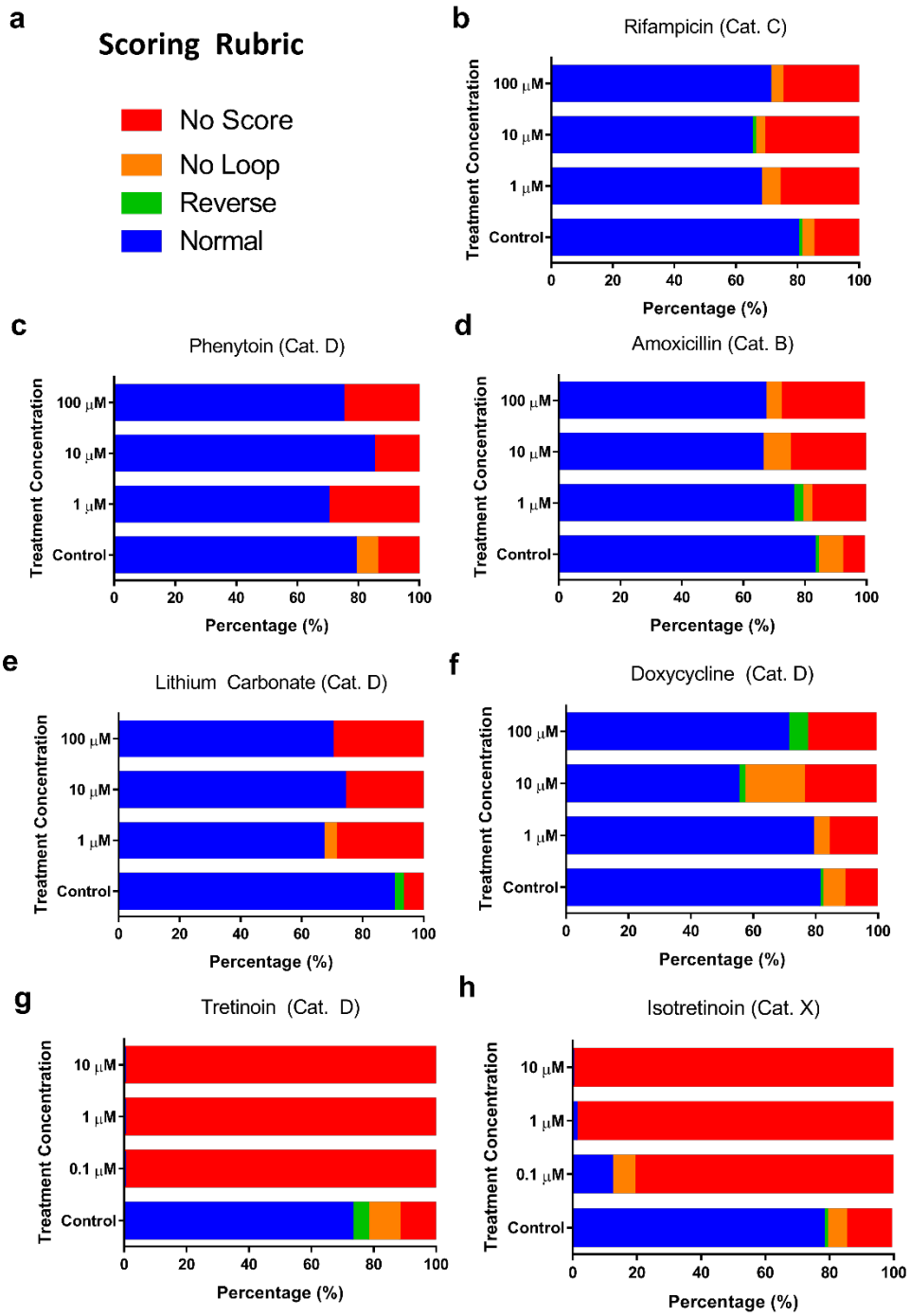

Supplemental Figure 7. *Zebrafish whole embryo culture (zWEC) assay of cardiac looping for seven drug compounds. (a) Morphological scoring was performed on heart structures of developing zebrafish embryos based on either normal (D-loop), reverse (L-loop), no loop, or no score where the heart did not express GFP and/or fall into the previous three categories. (b) Category C rifampicin and (c) Category D phenytoin produced mild developmental toxic effect. (d-f) Various drugs displayed moderate developmental toxicity amoxicillin (Category B), lithum carbonate (Category D), and doxycycline (Category D). Retinoids (g) Category D tretinoin and (h) Category X isotretnoin produced severe developmental toxic effects at all concentrations. (h) A sample size of n>19 embryos (pooled from 3 independent experiments) was used for all treatment groups.*

Supplemental Movies

Supplemental Movie 1. Three-dimensional confocal microscopy reconstructions of a cardiac organoids of 200 µm diameter (left), 600 µm diameter (middle), and 1000 µm diameter (right).

Supplemental Movie 2. Cross sectional reconstructions in z-direction of cardiac organoids of 200 µm diameter (left), 600 µm diameter (middle), and 1000 µm diameter (right).

Supplemental Movie 3. Cardiac organoids of 200 µm diameter (left), 600 µm diameter (middle), and 1000 µm diameter (right) exhibiting spontaneous contraction.

Supplemental Movie 4. Transient calcium flux of cardiac organoids of 200 µm diameter (left), 600 µm diameter (middle), and 1000 µm diameter (right).

Supplemental Tables

Supplemental Table 1. List of drug compounds with medicinal uses and previously designated pregnancy category.

Drug	Medicinal Use	Pregnancy Category	Concentrations Tested
Doxylamine Succinate	Antihistamine, sleeping aid	A	1 μM, 10 μM, 100 μM
Amoxicillin	Antibiotic (strep, middle ear infections etc.)	B	1 μM, 10 μM, 100 μM
Rifampicin	Antibiotic (TB, leprosy etc.)	C	1 μM, 10 μM, 100 μM
Lithium Carbonate	Bipolar antidepressant	D	1 μM, 10 μM, 100 μM
Phenytoin	Anticonvulsant	D	1 μM, 10 μM, 100 μM
Doxycycline	Antibiotic	D	1 μM, 10 μM, 100 μM
All-trans-RA (Tretinoin)	Acne treatment	D	0.1 μM, 1 μM, 10 μM
13-cis-RA (Isotretinoin)	Acne treatment	X	0.1 μM, 1 μM, 10 μM
Thalidomide	Myeloma, Inflammation	X	1 μM, 10 μM, 100 μM

Supplemental Table 2. List of primary and secondary antibodies used for immunofluorescent staining and imaging.

Primary antibodies (species)	Vendor	Catalog No.	Dilution
Cardiac troponin T (mouse)	Thermo Fisher Scientific	MS295P	1:200
Sarcomeric α-actinin (mouse)	Sigma-Aldrich	A7811	1:300
Myosin heavy chain (mouse)	Abcam	Ab97715	1:200
Cardiac troponin I (rabbit)	Abcam	Ab47003	1:200
Vimentin (mouse)	Thermo Fisher Scientific	MA5-11883	1:100
α-SM22 (rabbit)	Abcam	Ab14106	1:300
Calponin (rabbit)	Abcam	Ab46794	1:200
α-Smooth muscle actin (rabbit)	Abcam	Ab5694	1:100
OCT4 (rabbit)	Abcam	Ab18976	1:200
NANOG (mouse)	Thermo Fisher Scientific	MA1-017	1:100
SSEA4 (mouse)	Stem Cell Technologies	60062	1:200
SOX2 (rabbit)	Thermo Fisher Scientific	PA1-094	1:100
E-cadherin (mouse)	Abcam	Ab1416	1:200
Secondary Antibodies			
Alexa Fluor 488 goat anti-mouse	Thermo Fisher Scientific	A-11029	1:200
Alexa Fluor 546 goat anti-mouse	Thermo Fisher Scientific	A11003	1:200
Alexa Fluor 488 goat anti-rabbit	Thermo Fisher Scientific	A11008	1:200
Alexa Fluor 546 goat anti-rabbit	Thermo Fisher Scientific	A11010	1:200

Supplemental Table 3. TaqMan arrays used for cardiogenic and stromal gene expression analyses

Taqman Assay ID	Gene/Array Name	Taqman Assay ID	Gene/Array Name
Hs00153836_m1	ACVR1	Hs00276431_m1	NOX4
Hs00923299_m1	ACVR1B	Hs00383231_m1	NPPA
Hs00155658_m1	ACVR2A	Hs00173590_m1	NPPB
Hs00609603_m1	ACVR2B	Hs00176973_m1	PRKCA
Hs00181051_m1	APC	Hs00176998_m1	PRKCB
Hs00153179_m1	ATF2	Hs01090047_m1	PRKCD
Hs00394718_m1	AXIN1	Hs00178455_m1	PRKCE
Hs00205566_m1	BMP10	Hs00177010_m1	PRKCG
Hs00154192_m1	BMP2	Hs00702254_s1	PRKCI
Hs00370078_m1	BMP4	Hs00989970_m1	PRKCQ
Hs00233476_m1	BMP7	Hs00177051_m1	PRKCZ
Hs01034913_g1	BMPR1A	Hs01078066_m1	RB1
Hs00176144_m1	BMPR1B	Hs00195432_m1	SMAD1
Hs00176148_m1	BMPR2	Hs00183425_m1	SMAD2
Hs01026536_m1	CCNE1	Hs00929647_m1	SMAD4
Hs00372959_m1	CCNE2	Hs00195437_m1	SMAD5
Hs00154374_m1	CDC6	Hs00195441_m1	SMAD9
Hs00270923_s1	CEBPB	Hs00396596_m1	TBX20
Hs00193796_m1	CER1	Hs01052563_m1	TBX5
Hs00175141_m1	CHUK	Hs00413032_m1	TCF3
Hs00355045_m1	CTNNB1	Hs01009038_m1	TCF7L2
Hs00183740_m1	DKK1	Hs02339499_g1	TDGF1
Hs00737028_m1	DVL1	Hs00998133_m1	TGFB1
Hs00153451_m1	E2F1	Hs00234244_m1	TGFB2
Hs00231667_m1	E2F2	Hs01086000_m1	TGFB3
Hs00605457_m1	E2F3	Hs00610318_m1	TGFBR1
Hs00608098_m1	E2F4	Hs00234253_m1	TGFBR2
Hs00231092_m1	E2F5	Hs00182986_m1	WNT11
Hs00242501_m1	E2F6	Hs00263977_m1	WNT3A
Hs00266645_m1	FGF2	Hs00230534_m1	WNT8A
Hs00268943_s1	FZD1	Hs00610126_m1	WNT8B
Hs00273077_s1	FZD10	Hs00426835_g1	ACTA2
Hs00184043_m1	FZD3	Hs00901465_m1	CDH5
Hs00201853_m1	FZD4	Hs00959434_m1	CNN1
Hs00361869_g1	FZD5	Hs00164004_m1	COL1A1
Hs00171574_m1	FZD6	Hs00170014_m1	CTGF
Hs00275833_s1	FZD7	Hs00171584_m1	DLK1
Hs00259040_s1	FZD8	Hs00923996_m1	ENG
Hs00171403_m1	GATA4	Hs00911700_m1	FLK1
Hs01053355_m1	GNAI1	Hs00232764_m1	FOXA2
Hs01064686_m1	GNAI2	Hs00559473_s1	FOXC1
Hs00197803_m1	GNAI3	Hs00355202_m1	LGALS1
Hs00387073_m1	GNAQ	Hs01101425_m1	MYH6
Hs00255603_m1	GNAS	Hs04187281_m1	MYL4
Hs01564092_m1	GNB3	Hs00998018_m1	PDGFRA
Hs00275656_m1	GSK3B	Hs01065279_m1	PECAM1
Hs00231848_m1	HAND1	Hs01566750_m1	POSTN
Hs00232769_m1	HAND2	Hs00165814_m1	SOX9
Hs00167041_m1	HNF1A	Hs01038777_g1	TAGLN
Hs01001602_m1	HNF1B	Hs01385457_m1	TBX18
Hs00230853_m1	HNF4A	Hs00911929_m1	TBX2
Hs00212390_m1	LEF1	Hs00162646_m1	TCF21
Hs00745761_s1	LEFTY2	Hs00174816_m1	THY1
Hs00177373_m1	MAP3K7	Hs00165957_m1	TNNI3
Hs00176247_m1	MAPK14	Hs00943911_m1	TNNT2
Hs00231149_m1	MEF2C	Hs00958111_m1	VIM
Hs01110632_m1	MYH7	Hs01103751_m1	WT1
Hs00293096_m1	MYH7B	Hs99999905_m1	GAPDH (HK)
Hs00166405_m1	MYL2	Hs99999909_m1	HPRT1 (HK)
Hs00231763_m1	NKX2-5	Hs99999908_m1	GUSB (HK)
Hs00415443_m1	NODAL	Hs99999901_s1	18S (HK)

Experimental Procedures

Micropatterning of tissue culture surfaces

Surface micropatterning on tissue culture polystyrene was carried out using the selective etching approach described previously (Hoang et al., 2018). Patterned wafers were (SU8 master) fabricated using standard SU8 photolithography to fabricate molds with raised features of patterns. Poly(dimethyl siloxane) (PDMS) prepared at a 10:1 wt/wt ratio of elastomer base to curing agent was casted onto SU8 masters and clamped down using clear transparency sheets and glass slides. This process produced thin PDMS stencils with clear-through holes from the raised patterns on the SU8 master molds. Non-fouling poly(ethylene glycol) (PEG) solution was prepared by combining 150 mg PEG 1000 (Polysciences, cat. no. 16666), 1.8 mL PEGDA 400 (Polysciences, cat. no. 01871), 14.55 mL isopropyl alcohol, and 0.45 mL MilliQ water. The solution was grafted onto 6-well tissue culture plates and cured under UV light exposure (Dymax UV Illuminator; model no. 2000EC) for 45 seconds. Micropatterns were fabricated by selective oxygen plasma etching (Oxygen plasma treatment system, PlasmaEtch PE50XL) of the PEG using the PDMS stencils. Micropatterned tissue culture plates were sterilized by immersing in 70% ethanol for 1 hour and subsequent washing with sterile phosphate buffered saline (PBS).

Cell lines

Wild-type (WTC) hiPSC line was obtained from Dr. Conklin's laboratory at the Gladstone Institute of Cardiovascular Research. This hiPSC line was derived from a skin biopsy from a healthy adult Asian male donor in his early thirties. The original fibroblasts were reprogrammed using episomal methods with the factors of LIN28A, MYC (c-MYC), POU5F1 (OCT4) and SOX2. WTC GCaMPf6 hiPSC line was generated in Dr. Conklin's laboratory by targeting to the AAVS1 locus of WTC cells. A strong constitutive promoter (CAG) drives the expression of the GCaMP6f ORF. Yale-WT hiPSCs line was obtained from Dr. Abha Gupta's laboratory at the Yale University Department of Pediatrics and Child Study Center. Briefly hiPSCs were generated from the T-lymphocytes of a 25-year-old healthy South Asian male using the CytoTune-iPS Sendai Reprogramming kit as described previously (Liu et al., 2019).

Generation of cardiac organoids

Micropatterned surfaces were coated with diluted Geltrex hESC-qualified matrix (Life Technologies, cat. no. A1413302) at 37 ˚C for 1 hour prior to cell seeding. hiPSCs were cultured using standard PSC practices in Essential 8 (E8) medium (Life Technologies, cat. no. A1517001). At passaging confluency, cells were dissociated with Accutase (Life Technologies, cat. no. A1110501) and seeded at a density of $6.0x10^5$ cells per well of the micropatterned 6-well plate (~$0.63x10^5$ cells per cm^2) supplemented with 10 μM Y27632 (BioVision, cat. no. 1784-5). Cardiac differentiation was initiated approximately 3 days after seeding (Day 0) when the micropatterns reached confluency, and performed via small molecule modulation of the Wnt/β-catenin pathway (Lian et al., 2012) with GSK3 inhibitor CHIR99021 (Day 0) (Stemgent, cat. no. 04-0004) and WNT pathway inhibitor IWP4 (Day 2) (Stemgent, cat. no. 04-0036). Small molecules were diluted in in RPMI 1640 medium (Life Technologies, cat. no. 11875093) supplemented with B27-minus insulin (RPMI/B27 minus insulin) (Life technologies, cat. no. A1895601). Cardiac organoids began to contract around Day 9 of differentiation and were maintained in RPMI 1640 medium supplemented with complete B27 supplement (RPMI/B27 Complete) (Life Technologies cat. no. 17504044) until Day 20 for contractile and structural analysis.

Gene Expression Analysis

Gene expression was quantified using real-time qPCR analysis. On Day 20 of differentiation, cardiac organoids were sacrificed for RT-qPCR analysis. RNA was extracted using the RNeasy Mini Kit (Qiagen cat. no. 74104) and stored in -80 ˚C until needed. The RNA was then converted to cDNA using the Superscript IV First Strand Synthesis kit (Thermofisher cat. no. 18091050). Genes of interest includes cardiomyocyte-specific genes and stromal cell genes, plus TaqMan array of human factors for cardiogenesis (Thermofisher cat. no. 4414134). Individual genes are listed in the Supplemental Table 3. PCR plates were prepared and then run using the QuantStudio 3 Real-Time PCR System. All data was normalized to the respective housekeeping genes that were run in parallel with the rest of the gene assays. Value of ΔCt was

calculated by subtracting the average Ct of housekeeping genes from the Ct of the genes of interest. Lower ΔCt indicates gene upregulation, where high ΔCt indicates gene downregulation.

Flow Cytometry Analysis

Cardiac organoids were dissociated using 0.25% Trypsin for 10-15 minutes. Cells were collected, centrifuged and washed with PBS. Cells were fixed and permeabilized with a mixture of 4% (vol/vol) paraformaldehyde and 0.2% (vol/vol) TritonX solution for 15 minutes. Cells were incubated with primary antibody cardiac troponin T (Thermofisher cat. no. MA5-12960) in a 1:250 dilution for 1 hour in PBS, and then incubated with AlexaFluor 546 secondary fluorophore for an additional hour. The cell suspension was washed, centrifuged and filtered through 35 μm mesh cell strainer. Flow cytometry was performed on the BDAccuriC6 at Flow Cytometry Core at Syracuse University

Drug treatment

Concentrations were chosen after evaluation of blood plasma concentrations reported for each drug from the FDA drug information database (accessdata.FDA.gov). Concentrations were chosen to be at or approximated by blood plasma concentrations, while accounting for drug solubility in water or DMSO, while also supplying a large range in order to detect potential toxicity. Drugs were diluted in the appropriate culture media at three concentrations each increasing by a factor of 10 with respective controls. Control samples were supplemented with water or DMSO (≤ 0.1%), depending on the solvent used to prepare the concentrated stock. Once initiated, the drugs were supplied continuously throughout the differentiation into cardiac organoids in order to mimic the continuous drug exposure during fetal development. Samples were terminated on Day 20 for motion tracking analysis and for fluorescence/confocal imaging to assess the developmental toxicity of specific drugs based on the organoid morphology and contractile physiology.

Analysis of contraction physiology

Organoids were imaged in an onstage microscope incubator (OkoLab Stage Top Incubator, UNO-T-H-CO2) at 37 ˚C and 5% CO2 to maintain standard physiological conditions on a Nikon Ti-E inverted microscope with Andor Zyla 4.2+ digital CMOS camera. Videos of contracting cardiac organoids were recorded at 50 frames per second for ten seconds in brightfield and exported as a series of single frame image files. Contraction physiology was assessed using video-based motion tracking software (Huebsch et al., 2015) that computes motion vectors based on block matching of pixel macroblocks from one frame to the next. The motion vectors were assimilated into a contraction motion waveform representative of contractile physiology, providing metrics such as contraction amplitude and frequency. Peak-to-peak interval is the time interval between contraction peak and relaxation peak.

Contraction physiology was also assessed by recording the calcium transient using GCaMP6f hiPSC-derived cardiac organoids. Videos were taken under GFP excitation at 40 ms exposure time with 25 frames per second. Calcium flux signals were exported as Z-axis profiles in ImageJ. The fluorescence bleaching decay was corrected and time decay parameters τ_0, τ_{50}, τ_{75} were computed using in-house MATLAB scripts. The pulse duration is the time interval at which the calcium flux is at the half of the maximum flux. The time interval τ_0 is defined as the time it takes for the calcium flux to reach peak fluorescence intensity, whereas τ_{50} and τ_{75} represent the time it takes for the calcium flux to decay 50% and 75% of the peak fluorescence, respectively.

Relationships within the functional data was visualized utilizing R. Normalization to the zero mean, or Z-normalization, was utilized to normalize and scale each parameter to have a mean of 0 with a range near 1. This preprocessing step ensures allows us to study the correlation and similarities of our studied variables. t-Stochastic Neighbor Embedding (t-SNE), an unsupervised machine learning algorithm, was used for exploratory data analysis of the impact of pattern sizes on the measured variables of the organoids. This modern dimensionality technique is able to take high-dimensional data and reduce multidimensional relationships between data to a lower dimensional space in such a way that similar relationships are grouped

nearer to one another with a higher probability than dissimilar relationships or objects. This is accomplished by first creating a probability distribution of higher dimensional objects such that more similar pairs of higher dimensional objects are given a higher probability with more dissimilar points given a lower probability. A second probability distribution is then generated from this probability distribution for a lower dimensional map in such a way that preserves the maximum amount of similarity between the two probability distributions. t-SNE's ability to capture linear and nonlinear relationships between many variables makes it a powerful and versatile tool for investigating complex patterns while preserving higher dimensional structure of our data. t-SNE plots were generated using suggested parameters for perplexity (van der Maaten and Hinton, 2008), in order to condense the relationships between multiple recorded parameters down to a two-dimensional representative plot. Measurements were collected from mean values collected from 166 organoids. The actual t-SNE analysis was performed in R utilizing Jesse Krijthe's 2015 package Rtsne: T-Distrubed Stochastic Neighbor Embedding using a Barnes-Hut Implementation (https://github.com/jkrijthe/Rtsne) to reduce the representation of our parameters to two dimensions. Pattern diameters were displayed by varying size and color of each point, and then individual parameters were investigated by applying a color gradient in the t-SNE plots. A heatmap of the same data was generated to visualize each variables impact with respect to pattern diameter concurrently (Gu et al., 2016), while a correlogram gives further insight into the impact between parameters (Wei et al., 2017) by utilizing Frank Harrell's Hmisc package to generate these figures https://CRAN.R-project.org/package=Hmisc.

Immunofluorescence staining and confocal microscopy

Organoids were characterized based on immunofluorescence staining patterns of cardiac tissue and smooth muscle-like tissue. After video recording, samples were sacrificed and fixed with 4% (vol/vol) paraformaldehyde (PFA) for 10 minutes. After PFA treatment, samples were washed and permeabilized with 0.2% (vol/vol) Triton X-100, blocked with 2% (wt/vol) bovine serum albumin (BSA) and incubated with the appropriate dilution of primary antibodies for 1 hour at room temperature. After incubation, the

primary antibody was removed and washed with PBS. Secondary fluorescent antibodies were then incubated in the dark for 2 hours at appropriate dilutions and nuclei were tagged with 300 nM DAPI. All primary and secondary antibodies used are listed in Supplemental Table 2. Confocal microscopy (Zeiss U880) was used to capture z-stacks (8 μm spacing between slices) of the organoids for height measurements and 3D reconstruction.

Morphological and structural characterization of cardiac organoids

The cardiac organoids were assessed based on three parameters that characterize the overall cardiac tissue distribution and 3D morphology (Supplemental Fig. 2). All images were imported into ImageJ for image reconstruction and analysis. The *Area Ratio* was measured by using the circular or elliptical tool to approximate the area of fluorescence of tissue staining positive for cardiac tissue, and normalizing this area relative to the area of the entire pattern. The *Height* was measured by locating the top and bottom of the organoids using confocal microscopy. Lastly, the *FWHM* was determined by measuring the tissue diameter at half of the organoid height.

Zebrafish whole embryo culture (zWEC) embryotoxicity assay

Transgenic *Tg(myl7:GFP)* zebrafish that express GFP exclusively in cardiomyocytes were used to observe myocardium development *in vivo* (Huang et al., 2003). Adult fish were bred to generate a few hundred synchronized embryos, which were divided into individual wells of approximately 50 embryos. The drug stocks were diluted in zebrafish embryo medium. Chemicals at the same concentrations described in Supplemental Table 1 were administered to chorionated zebrafish embryos within the first 5 hpf, which is the estimated equivalent to the time point when the chemicals are introduced to the human cardiac organoids. Fresh embryo medium with chemicals is replaced at 24 hpf, when the embryos have developed a prominent linear heart tube, but not yet undergone looping. At 48 hpf, cardiac morphology and looping were scored as the first assessment of cardiac developmental toxicity on *in vivo* organogenesis. zWEC embryotoxic potentials of each chemical were scored based on the percentage of embryos exhibiting distinct

cardiac morphology at 48 hpf. Normal looping (D-looping) refers to looping to the right-hand side of the embryo. Reverse looping (L-looping) is classified as looping towards the left side of the embryo, while no looping (N-looping) refers to a straight linear heart tube that has not successfully undergone cardiac looping events. A subset (~20%) of embryos, including controls, did not express the GFP transgene, potentially due to silencing, and therefore cannot be classified as D/L/N-looping in this assay. Treatments that produced a rate of GFP absence that was significantly higher than controls are considered to reflect a severe abnormality in myocardial development.

Statistical Analysis

Data was plotted as box plots or mean ± s.d. For single comparisons between two individual groups, a two-sided Student's t-test was used, and $p \leq 0.05$ was considered significant. For comparisons between more than two groups, one-way analysis of variance (ANOVA) was performed and $p \leq 0.05$ was considered significant. ANOVA analysis was supplemented with multiple comparison tests to determine significance between groups.

References

Gu, Z., Eils, R., and Schlesner, M. (2016). Complex heatmaps reveal patterns and correlations in multidimensional genomic data. Bioinformatics *32*, 2847–2849.

Hoang, P., Wang, J., Conklin, B.R., Healy, K.E., and Ma, Z. (2018). Generation of spatial-patterned early-developing cardiac organoids using human pluripotent stem cells. Nat. Protoc. *13*, 723–737.

Huang, C.J., Tu, C.T., Hsiao, C. Der, Hsieh, F.J., and Tsai, H.J. (2003). Germ-line transmission of a myocardium-specific GFP transgene reveals critical regulatory elements in the cardiac myosin light chain 2 promoter of zebrafish. Dev. Dyn. *228*, 30–40.

Huebsch, N., Loskill, P., Mandegar, M.A., Marks, N.C., Sheehan, A.S., Ma, Z., Mathur, A., Nguyen, T.N., Yoo, J.C., Judge, L.M., et al. (2015). Automated Video-Based Analysis of Contractility and Calcium Flux in Human-Induced Pluripotent Stem Cell-Derived Cardiomyocytes Cultured over Different Spatial Scales. Tissue Eng. Part C Methods *21*, 467–479.

Lian, X., Hsiao, C., Wilson, G., Zhu, K., Hazeltine, L.B., Azarin, S.M., Raval, K.K., Zhang, J., Kamp, T.J., and Palecek, S.P. (2012). Robust cardiomyocyte differentiation from human pluripotent stem cells via temporal modulation of canonical Wnt signaling. Proc. Natl. Acad. Sci. *109*, E1848–E1857.

Liu, W., Dong, W., Hoffman, E.J., Fernandez, T. V, and Gupta, A.R. (2019). CHD8 regulates the balance between proliferation and differentiation of human iPSCs in neural development. bioRxiv 732693.

van der Maaten, L., and Hinton, G. (2008). Visualizing Data using t-SNE. J. Mach. Learn. Res. *9*, 2579–2605.

Wei, T., Simko, V., Levy, M., Xie, Y., Jin, Y., and Zemla, J. (2017). Visualization of a Correlation Matrix. Statistician *56*, 316–324.